THROUGH-THE-THICKNESS MATERIAL PROPERTIES IDENTIFICATION USING 3D DIC AND FBG MEASUREMENTS

Matthieu Mulle [1], Redouane Zitoune [1], Francis Collombet [1], Philippe Olivier [1], Laurent Robert [2], Yves-Henri Grunevald [3]

[1] *Laboratoire de Génie Mécanique de Toulouse, Equipe PRO²COM, IUT Paul Sabatier Dépt. GMP, 133c av. de Rangueil, 31077 Toulouse cedex 4*
matthieu.mulle@iut-tlse3.fr; redouane.zitoune@iut-tlse3.fr; francis.collombet@iut-tlse3.fr
[2] *CROMeP, Ecole des Mines d'Albi Carmaux, 81013 Albi CT cedex 09*
laurent.robert@enstimac.fr
[3] *DDL Consultants, Pas de Pouyen, 83330 Le Beausset*
ddl.consultants@wanadoo.fr

ABSTRACT

The present study is an analysis of the central reinforced zone of a carbon epoxy technological specimen in terms of initial state and mechanical behaviour. For this, several optical fiber Bragg grating sensors (FBG) have been embedded and spread through-the-thickness of the thick zone. The first step concerns the autoclave cure monitoring during when distribution and amplitudes of residual strains are estimated. A through-the-thickness strain gradient appears which is assumed to result from mould-part interactions. The specimen is then submitted to reheating tests in order to determine the thermal expansion behavior of the reinforced zone. Through-the-thickness variable thermal elastic properties are observed. Results are compared with both autoclave cure measurements and a numerical simulation. Discrepancies observed highlight the influence of environmental effects. In a second step, the technological specimen is submitted to 3 and 4-point bending tests in order to estimate strain distribution during solicitations. Measurements are obtained with both FBG and 3D digital image correlation (3D-DIC). Both techniques show a general linear distribution of through-the-thickness longitudinal strains but values are slightly different. A numerical model is developed and a test-calculation dialogue is carried out to identify material properties. The combination of embedded and surface measurements reveals the importance of considering structural effects.

KEYWORDS: technological specimen, fiber Bragg grating sensors, autoclave cure monitoring, residual strains, strain field, 3D digital image correlation.

1. INTRODUCTION

Designing composite structures runs up against obstacles related to the multiplicity of the involved scales, to the complexity of the mechanical response, to the lack of knowledge on the material state in the structure and also to the variability of the properties induced by the various manufacturing phases. Classically, the material properties are identified starting from tests carried out on elementary specimens. This step is the base of the building block (pyramid of tests) procedure. However, taking into account the differences in scale between elementary specimens and industrial structure, the identification of the material parameters only have some sense if the response of the composite material is studied within the structure [1, 2].

This property identification procedure, is an essential subject of the French national research program called AMERICO (Multi-scale analysis of composite materials), conducted by the ONERA (French Aerospace Lab) [3]. This program aims at defining methods for multi-scale analysis and design of composite structures. In this framework we worked on a cross-linked experimental/calculation approach based on the development and the study of a technological specimen. This specimen is an object which relates the elementary coupon to the industrial structure. It is of beam type and contains design singularities such as important thicknesses, ply drop off zones and a reinforced zone (fig. 1, 2 and 3). The material analysis in this structure is obtained thanks to the strategic incorporation of optical fiber Bragg gratings (FBGs) sensors in

the specimen's core. The present study concerns the analysis of the central reinforced zone of the specimen where several FBGs have been embedded and spread through-the-thickness. The first step concerns the autoclave cure monitoring of the carbon epoxy (Hexply M21 T700GC) technological specimen obtained thanks to the FBG's [4, 5, 6, 7, 8]. Distribution and amplitudes of process induced strains are estimated. After cure, the specimen is submitted to a series of reheating tests in an oven in order to determine the thermal expansion behavior of the reinforced zone [9]. The heating procedure corresponds to the cure cycle, replacing the material under conditions close to that of its birth (stress free temperature). A numerical model (FEM) is developed to simulate the reheating tests. Thermal strains are predicted. Experimental results are analyzed before being compared to theoretical results. Some discrepancies are observed and raise questions related to environmental and structural influences.

In a second step, the mechanical behavior is analysed through a series of 3 and 4-point bending tests. We are interested in the stain gradients and the presence of shearing in the central reinforced zone of the technological specimen. The strain distribution during solicitations is obtained with both FBGs [10] and 3D digital image correlation (3D-DIC). To date, the capacity of FBG embeddment in laminates has not been much exploited to study through-the-thickness strain distributions. To our knowledge only Du [11] and Bosia [12] have studied this aspect using fiber Bragg gratings. They have both used laminated plates which were subjected to 3 point bending tests. The first one showed a very satisfactory correlation between experimental and theoretical results. The second one focussed his analysis on the effect of load concentration (under the point of application) over the FBG information. Our approach is different. It consists in studying the influence of important thicknesses and structural effects on the strain distribution taking care that our measurements are the more reliable possible. In this objective, the 4-points bending test is particularly interesting. Indeed, it allows the study of a zone situated between the 2 central points of application, where the effect of shearing is minimized and where in the same ply the axial deformation is constant. Under these conditions, there should be no strain gradient along the FBG and axial errors of sensors positioning should have no influence. The use of the 3-D DIC technique in this work brings an interesting added value. It will first help to verify the above assumptions by examining strain fields in the sensor corresponding areas. It will also provide a complementary technique to measure strains on the surface and particularly shear strains. A test-calculation dialogue is then undertaken [13].

The first sections of this paper give descriptions of the technological specimen and its instrumentation, optical measurement techniques and numerical model. The following sections concern the analysis of the experimental results and the comparison with the numerical simulations.

2. EXPERIMENTAL

2.1 Technological specimen

The technological specimen is of beam type whose length/width ratio is 10. It contains a central reinforced zone and thus a ply drop off at each end of the reinforced zone. It is intended to represent the skin of a plane wing with a local reinforcement likely to support a load by a bolted assembly. The reinforced zone consists of an addition of plies in the form of a patch, sandwiched between two half thicknesses of the thin zone. These specimens are manufactured per series of 16 out of the same mother plate. After the autoclave cure, specimens are cut out by abrasive water jet machining. Dimensions are presented in figure 1.

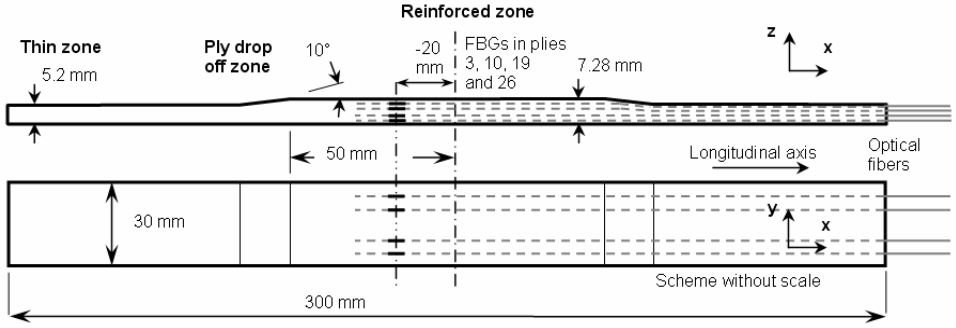

Figure 1. Plan of the technological specimen. Dimensions and FBG instrumentation.

Specimens are made with a carbon/polymeric Hexply M21 T700 (reference: M21 / 35 % / 268 / T700GC) pre-preg manufactured by Hexcel Composites. They are cured at 180°C during 2 hours under 7 bar pressurization and -0.7 bar vacuum. The M21 matrix combines a thermoset epoxy with thermoplastic phases (in both liquid and solid phases). The carbon fibers are the Toray T700GC. As for the ply stack, it is a typical aeronautical sequence (cf. fig. 2). Specimens are made of 20 plies in the thin lateral zones (5.2 mm thick) and of 28 plies in the reinforced zone (7.28 mm thick). The thin zone has the following reinforcement distribution: 50 % at 0°, 40 % at +/-45° and 10 % at 90°. The reinforced central zone has a complementary embedded patch which has the following reinforcement distribution: 25 % at 0°, 50 % at ± 45° and 25 % at 90°.

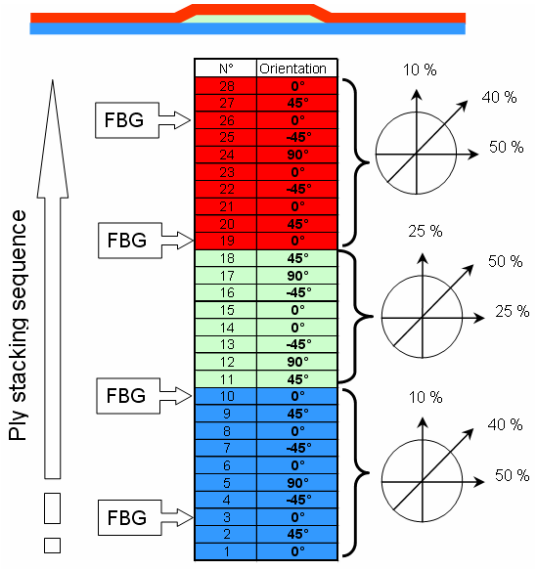

Figure 2. Ply stacking sequence of the technological specimen and position of embedded FBGs.

2.2 Instrumentation

- **FBGs**

Their working principle was detailed in various papers in the last decade [9-11]. They are mainly sensitive to temperature (T) and axial strains (ε_{xx}) and deliver information which is related to a variation of the Bragg wavelength ($\Delta\lambda_B$) as shown in eq. 1.

$$\frac{\Delta\lambda_B}{\lambda_B} = a\Delta T + b\varepsilon_{xx} \qquad (1)$$

Coefficients *a* and *b* depend on the nature of the optical fiber silicate and the FBG inscription parameters and are determined through a calibration procedure. During non constant temperature conditions the corresponding component of eq. 1 is obtained thanks to thermocouples. They are embedded in the mother plate sufficiently far from the FBG so that it does not affect the specimen's mechanical behavior, but in similar conditions in order to sense identical heat changes during the curing process.
For this study FBGs employed are written in standard SMF28 single mode optical fiber. Four FBGs have been embedded through-the-thickness of the reinforced zone during the pre-preg lay up. They are positioned 20 mm from the longitudinal center of the specimen, in plies 3, 10, 19 and 26, as shown in figures 1 and 2.
A MicronOptics si425 Bragg wavelength interrogator is used for the autoclave cure monitoring, the reheating tests as well as for the bending tests.

- **3-D DIC**

The 3-D DIC method is based on both digital image correlation (DIC) and stereovision, and was developed at the end of the last century. The technique uses a DIC algorithm to determine point correspondences between two images of a specimen acquired from two rigidly bounded cameras. The correlation scores are computed by measuring the similarity of a fixed subset window in the first image to a shifting subset window in the second one. A first order two-dimensional shape function in the subset and a zero normalized sum of square difference (ZNSSD) correlation criterion are used. Sub-pixel correlation is performed using quintic B-spline grey level interpolation. After determining the calibration parameters for each camera as well as the 3-D relative position/orientation of the two cameras (pinhole model and radial distortion of 3rd order), the 3-D specimen shape can be reconstructed from the point correspondences using triangulation. To determine the 3-D displacement field, DIC is also used to determine point correspondences between the stereo pairs acquired before and after deformation. The strain field is obtained from the displacement field by numerical differentiation. A complete description of the 3-D DIC technique can be found in the literature, e.g. Luo et al. [14] or Synnergren et al. [15].

For this study, in order to capture identifiable images, a randomly distributed paint pattern is laid on the side of the technological specimen at a position corresponding to FBGs projection (ie. the side of the central reinforced zone).

3. NUMERICAL MODEL

This study is carried out by means of the finite element SAMCEF software. Three-dimensional laminated finite element of type 11 is used with degree 1 and 33 degrees of freedom (24 + 9 incompatible) each, available in the SAMCEF software library. The model is composed of 3 elements in the central (thick) zone (10 plies per element) and 2 in the current (thin) zone (8 plies per element). It involves 1040 elements representing 6264 degrees of freedom.
For the reheating test simulation the specimen is modelled on a metallic mould. The mould/laminate interface is modelled with friction free contacts. A stain gradient of -155°C is imposed to the specimen and the mould in order to simulate the cooling phase of the process. For the bending tests simulation the loading is carried out with imposed displacements. Finally, it must be pointed out that the initial set of mechanical properties used in these simulations was identified through a series of standard tests, using elementary coupons.

4. RESULTS AND DISCUSSIONS

4.1 Autoclave cure strain assessment

The longitudinal strain changes during the cure cycle are presented in figure 3 in various plies of the reinforced zone. The optical fibers and its FBG sensors detect the axial strains which the composite undergoes at the vitrification point, i.e. at the first third of the curing dwell. Strain changes decrease very slightly until the end of the dwell.

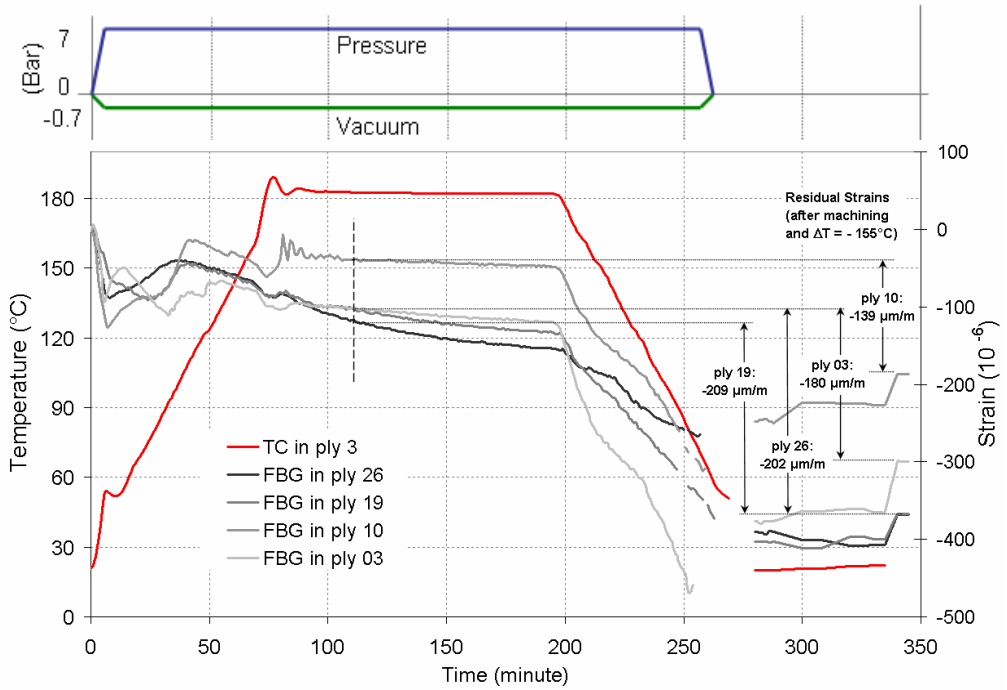

Figure 3. Process induced strain changes measured by FBGs through–the-thickness of the reinforced zone of the technological specimen during the autoclave cure cycle.

At the beginning of the cooling phase strains progress negatively. This is in agreement with the thermomechanical behaviour of this laminate but in fact the contraction is amplified by that of the metal mould. Indeed, after the end of the temperature cooling and after the laminate was released from the mould (lack of acquisition in the graph), the reinforced zone was let free to expand. During this cooling, one also notes that the curves take different orientations from one ply to the other. That implies that the material does not behave in the same manner according to the position in the thickness. After release from the mould and cutting of the specimens, residual cure strains are estimated. Results are indicated on figure 3. A nonlinear gradient through-the-thickness is noted. It is supposed that this gradient is not linear because of the shape of specimen or the incorporation of a patch in the ply stack. The tool/part interactions which took place at the time of the cooling phase must also be considered as a responsible factor to these deformation differences. This information is important because it reveals a variability of thermal properties in the thickness of the technological specimen. It highlights the importance of characterizing the material within the structure.

4.2 Thermal strain assessment during the reheating process

After having been the subject of a first analysis at the time of the autoclave cure, the specimen is subjected to a thermo mechanical analysis. The idea is to study the strain distribution of thermal origin through-the-thickness of the specimen during a thermal test in an oven. The analysis conditions are less complex than those of the curing process since the specimen is subjected only to the temperature parameter (no pressure, no vacuum, no chemical transformation…). The temperature cycle is equivalent to that of curing, with the difference that when the 180°C dwell is reached, this one lasts only 30 minutes, instead of 120 minutes. It is considered that the most important is to replace the specimen under thermal conditions of birth (i.e. 180°C) and that a prolongation of these conditions does not bring additional information. The cooling phase is different from that of the autoclave process as no cooling control is available except by

ventilation. As this is not sufficient, the oven is opened to accelerate cooling as much as possible.
The evolution of strains in plies 3, 10, 19, and 26 according to the temperature cycle are presented in figure 10. The strain changes are very similar to that of the temperature. It is noted however that according to the position through-the-thickness of the reinforced zone of the specimen, strains do not evolve with the same intensity. Once the isothermal dwell is reached, one observes various strain levels which recalls those observed during the curing process. The residual thermally induced strain in plies 3, 10, 19, and 26 are estimated and gathered in table 1. Strain distributions are very similar from those obtained during the autoclave cure process (cf. fig. 3). There is thus a typical distribution since reproducible. This means that we have a variability of thermal elastic properties within the structure. These properties are elaborated during the cure cycle and are fixed in the material.

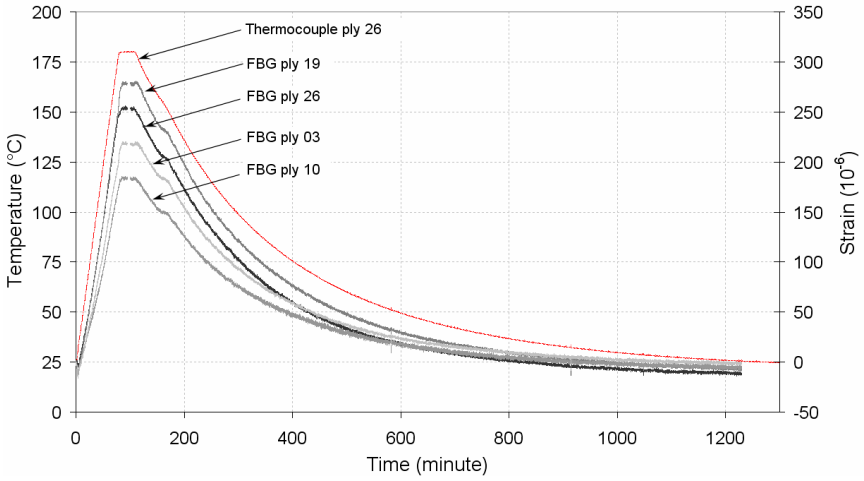

Figure 4. Thermally induced strain changes measured by FBGs through-the-thickness of the reinforced zone of the technological specimen during the oven reheating cycle.

If the strain gradient shapes are similar, amplitudes differ by approximately 25 %. One can think that the material properties changed with time. Environmental effects such as moisture absorption or other ageing parameters are certainly responsible for these discrepancies.

4.3 Comparison with the heating test simulation

The numerical results obtained by FEM are presented in table 1 jointly with the two series of experimental results. One can thus compare the numerical results with the autoclave cure residual strains and the thermally induced strains. Initially, it is noted that the distributions resulting from the experimental tests are different than those obtained numerically. Only in the last case is there a quasi-linear strain gradient. Obviously, calculation does not take into account the variation of the thermal elastic properties since only one longitudinal expansion coefficient was introduced into the numerical model. Consequently, results reveal only a very light strain gradient. The difference observed may also be attributed to the structural effect underlined above.
The calculated residual strain intensities are very different from those measured at the time of the reheating procedure (variation of 35 % in ply 26) whereas they are closer to those measured at the time of the autoclave curing process (variation of 4 % in ply 26). This contributes towards the analysis of section 4.2. Indeed, the material right after cure does not have time to undergo the effects of the environment and for this reason, its behavior is rather close to that of the numerical simulation.

	Autoclave cure		Oven reheating procedure		Numerical simulation
	Bragg gratings ε_{xx} (10^{-6})	Variation / Num. sim. (%)	Bragg gratings ε_{xx} (10^{-6})	Variation / Num. sim. (%)	ε_{xx} (10^{-6})
Ply n° 26	-202	4	-264	35	-195
Ply n° 19	-209	11	-280	49	-188
Ply n° 10	-139	-23	-189	5	-180
Ply n° 3	-180	2	-212	20	-176

Table 1. Through-the-thickness ε_{xx} strain values obtained by numerical simulation and measurements during autoclave cure and reheating procedure of the technological specimen.

4.4 Strain distribution during bending tests

- **Observations and analysis**

We remind to the reader that for the reasons explained in the introduction of this paper the study starts with the 4-point bending test series (cf. figure 5a).

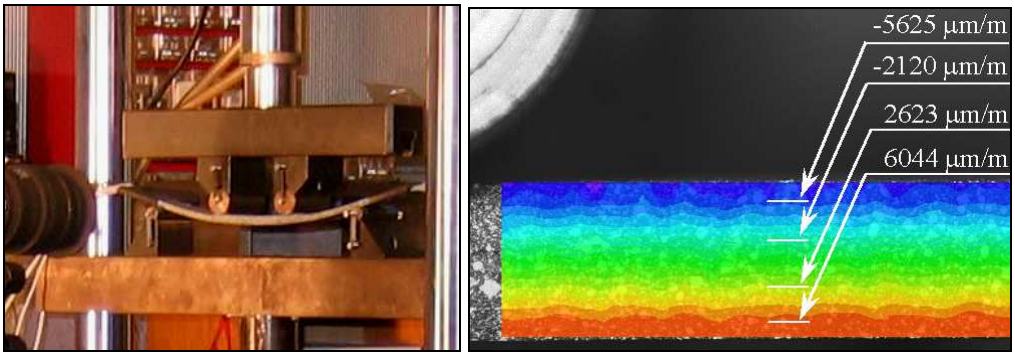

Figure 5. a) Multi-instrumented technological specimen submitted to a 4-point bending test. b) 3D DIC longitudinal strain field in the reinforcement zone for a 16 mm displacement

Results are first analysed at a global scale (scale of loading, cf. fig.6). Compared to the efforts calculated numerically according to the central displacement, experimental results show a linear evolution up to 10 mm displacement. Until there, the discrepancy observed is roughly 6 %.

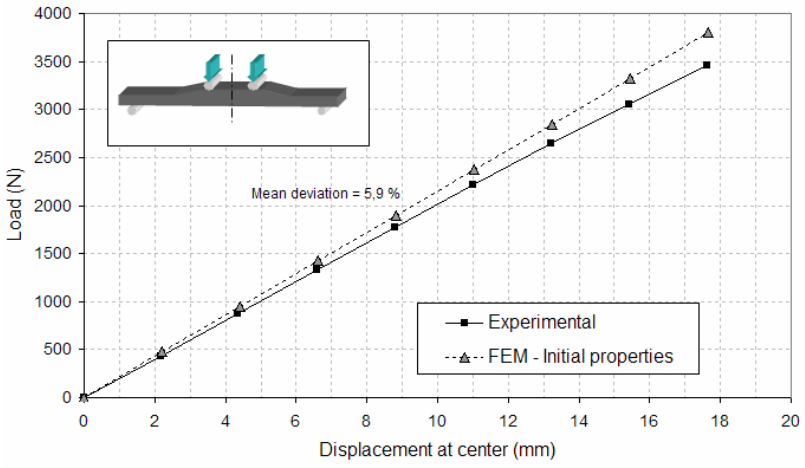

Figure 6. Load changes versus displacement for the 4-point bending test. Test – calculation comparison

Beyond a 10 mm displacement, an inflection is observed and the deviation with the numerical curve increases. This is explained by the geometrical nonlinear behavior and/or the material of the solicited specimen which is not taken into account by the model. Results are then analyzed at the local scale (scale of strains). Figure 5b presents the ε_{xx} strain fields measured by stereo-correlation in the reinforced zone (between the central loading cylinders), for a 16 mm displacement. The lines on the image correspond to the projection of the active part of the 4 FBG sensors (in core) on the specimen lateral side. For a more detailed observation, figure 5b presents the longitudinal strain distribution along these lines, over a length of approximately 10 mm. One notes a relatively good uniformity of the longitudinal strains in the same ply and thus along the FBG. These strains values may then be averaged over the FBG length, in order to be compared with FBG measurements and numerical results.

In figure 7, through-the-thickness strain distributions (delivered by both measurement techniques and calculation (FBG, 3-D DIC MEF) are revealed by a graphic construction which connects each measurement point. Various displacements are considered. Each technique shows an overall linear behavior. However, the built lines do not present the same slopes. The distribution lines obtained by 3-D DIC for 4 displacements cross in the same point, but this one is different to those obtained with FBG measurements and FEM calculations. For these last the intersection point is closer to the theoretical neutral axis. Strains measured by 3-D DIC only match correctly in the lower part of the specimen (solicited in tension). In the upper part (solicited in compression) one observes some discrepancies of approximately 5% in the worst case (ply 26 for a 16 mm displacement).

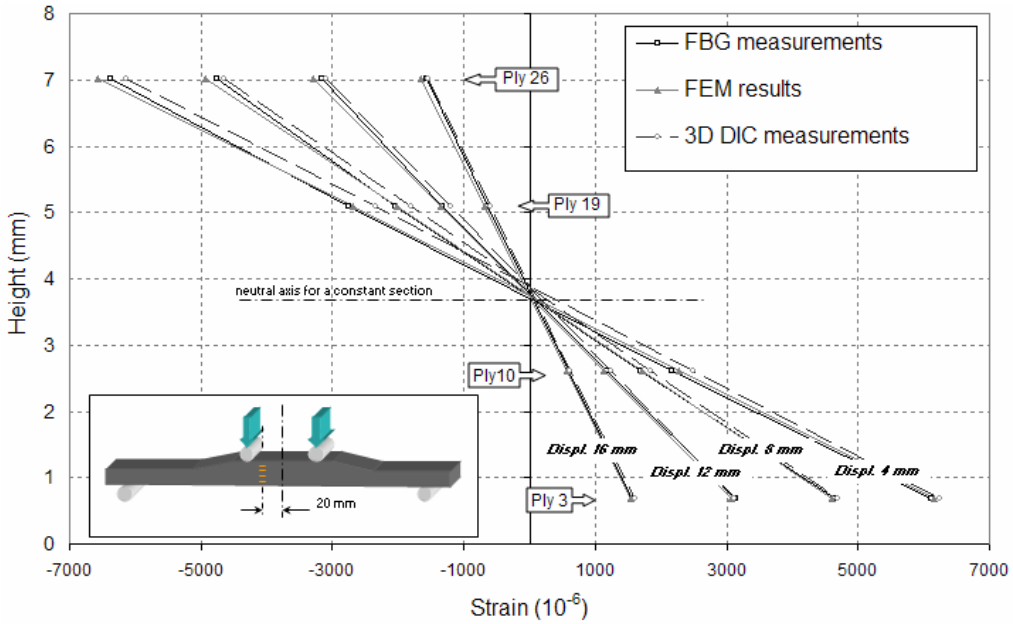

Figure 7. Through-the-thickness strain distribution for displacements of 4, 8, 12 and 16 mm. Comparison between FBGs, 3D-DIC, and FEM.

- **Test-calculation dialogue**

In the following step, a test-calculation dialogue is established to identify a set of properties which allows a correlation as close as possible with measurements obtained on the global scale (scale of loadings) then local (scale of strains). Properties are "adjusted" within the framework of the 4-points bending test. As shear stresses are minimized in between the 2 central points of application, we essentially act on compression and tension modules. In an iterative way, the material properties are adjusted until an acceptable maximum difference of 5 % between numerical results and experimental measurements is reached. The pair of modules retained is

the following: ELt = 113 GPa for 12.8 % variation with the initial module, and ELc = 105 GPa for 11.7 % variation with the initial module.
The numerical model and its associated parameters are now used to simulate the 3-point bending test. At the global scale, the numerical results show a good agreement with the experimental values. At the local scale of strains, significant variations are noted for the external plies (about 18 %). For the inner plies, the variations are lower. These differences may come from possible inaccuracies in sensors longitudinal positions. Such miss positioning has an influence for this mode of solicitation since strains are not constant along the same ply. We point out that for the 4-points bending test this problem does not arise because strains are quasi-constants in the same ply between the central points of load application.
Another assumption can explain the origin of these variations. It relates to not taking into account the shear modulus in the 4 points bending test-calculation dialogue. Indeed, an analysis of the shear strain fields by 3-D DIC shows a non negligible presence of a shearing effect. This effect probably results from the non linear geometry of the specimen. Adjusting the shear modulus in the 4 point bending test-calculation dialogue is thus necessary so that the resulting fitted properties may be used with improved efficiency to simulate the 3-point bending test.

5. CONCLUSION

The central reinforced zone of a carbon epoxy technological specimen is instrumented through-the-thickness with embedded FBGs. Process induced strains are assessed during the autoclave cure and then during reheating tests of similar temperature cycle. Both series of experimental results show identical residual strain distribution. A non linear gradient is observed revealing thermal properties variability through-the-thickness of the structure. Both mould/laminate interactions and structural effects (presence of a reinforcement patch) are considered influent. As for the strain intensities they show a mean 25 % discrepancy. This may be due to humidity and/or relaxation effects.
A numerical model (FEM) is developed to simulate the reheating tests. The strain distribution is linear and shows almost no gradient. Introducing only one thermal coefficient in the model is thus not sufficient to represent the material behavior. The strain values are however closer to those related to the autoclave cure. This is logical since the numerical simulation did not consider any effects induced by environmental parameters.
The specimen is submitted to 3 and 4-point bending tests. Those are accompanied by 3D digital image correlation strain field measurements which bring complementary global information gathered on the surface. Both techniques show a general linear distribution of through-the-thickness longitudinal strains. A test-calculation dialogue is carried out in the frame of the 4-point bending test. In an iterative way, the material properties are first adjusted at a global scale (effort scale) and then at a local scale (strain scale). As the analysed zone is in between the 2 central bearings, adjusting the shear modulus has almost no impact on the correlation procedure. It's mainly Young's moduli in the tensile and compressive directions that are adjusted. The numerical model and its associated parameters are used to simulate the 3-point bending test. A satisfactory correlation is observed with experiment as far as the effort scale is concerned. At the local scale some discrepancies appear highlighting the need to adjust the shear modulus. Indeed, returning to the 4-point bending, non negligible 3D-DIC shear strain fields are observed in the central zone. The study shows the complementarities of embedded and surface measurements. It also shows how these techniques contribute to the identification of the material properties and variabilities underlining the importance of considering the material within the structure.

Acknowledgements

The authors wish to thank DDL Consultants Company for its technical support and for financing a thesis concerning this project, the DGA (Direction Générale de l'Armement) for its

financial support through the upstream program AMERICO and HEXCEL Composites Company for providing us with HexPly® pre-preg.

REFERENCES

1. Grunevald Y.-H., Collombet F., Mulle M., Ferdinand P., "Global approach and multi-scale instrumentation of composite structures in the field of transportation", proceedings of 8th Japan Int. SAMPE Symposium, Tokyo (Japan), Vol. 2, 2003, p. 665-675.
2. Grunevald Y.-H., Collombet F., Mulle M., "Integrated approach for designing composite structures: a new industrial challenge", invited lecture of 34th Solid mechanics Conference, Zakopane (Poland), 27-28, September 2-7 2002, volume of abstracts published by Atos Poligrafia-Reklama for IPPT polish Academy of Sciences.
3 Laurin F., Carrère N., Maire J.-F., "A multiscale progressive failure approach for composite laminates based on thermodynamical viscoelastic and damage models", Composite Part A, 2007, 28, 198-209.
4. Okabe Y., Yashiro S., Tsuji R., Mizutani T., Takeda N., "Effect of thermal residual stress on the reflection spectrum from fiber Bragg grating sensor embedded in CFRP laminates", *Composites Part A*. 2002, Vol. 33, pp. 991-999.
5. Guemes J. A., Menéndez J. M., "Response of Bragg grating fiber-optic sensors when embedded in composite laminates", Composites Science and Technology, Issues 7-8, 2002, Vol. 62, pp. 959-966.
6. Kuang K.S.C., Kenny R., Whelan, M.P., Cantwell, W.J., Chalker P.R., "Embedded fibre Bragg grating sensors in advanced composite materials ", Composites Science and Technology, 2001, 61, 1379-1387.
7. Leng, J.S., and Asundi, A., "Real-time cure monitoring of smart composite materials using extrinsic Fabry Perot interferometer and fiber Bragg grating sensor", Smart materials and structures, 2002, Vol. 11, pp. 249-255.
8. Lawrence, C.M., Nelson, D.V., Spingarn, J.R., and Bennett, T.E., "Determination of process-induced residual stress in composite materials using embedded fiber optic sensors", in: Proceedings of SPIE, K.A. Murphy and D.R. Huston Editors, Smart structures and materials. 1997: smart sensing processing and instrumentation. 1997, Vol. 3042: pp. 154-165.
9. Mulle, M., Collombet, F., Périé, J.-N., and Grunevald, Y.-H., "Instrumented technological specimen (its): curing process and mechanical characterization using embedded fiber Bragg gratings", Proceedings of the 11th ECCM, Rhodes, Greece, paper #C137, 2004.
10. Mulle M., Zitoune R., Collombet F., Olivier P., Grunevald Y.-H., Thermal expansion of carbon–epoxy laminates measured with embedded FBGS – Comparison with other experimental techniques and numerical simulation", Composites: Part A 38 (2007) 1414-1424.
11. Du W., Tao X.M., Tam H.Y. et Choy C.L., "Fundamentals and applications of optical fiber Bragg grating sensors to textile structural composites", *Composite Structures*, 42, 217-229, 1998.
12. Bosia F., Fachini M., Botsis J., Gmür T., De'Sena D., "Through-the-thickness distribution of strains in laminated composite plates subjected to bending", *Composite Science and Technology*, 64, pp. 71-82, 2004.
13. Collombet F., Mulle M., Grunevald Y.-H., and Zitoune R., "Contribution of embedded optical fiber with Bragg gratings in composite structures for test-simulation dialogue, *Mechanics of Advanced Materials and Structures*, Vol.13, Number 5, pp. 429 – 439, 2006
14. Luo P., Chao Y., Sutton M., Peters W., Accurate measurement of three-dimensional deformations in deformable and rigid bodies using computer vision. Exp Mech 30(2): 123–132, 1993.
15. Synnergren P., Sjödahl M., A stereoscopic digital speckle photography system for 3-D displacement field measurements. Opt Lasers Eng 31, 425–443,1999.